

“Spin orders” in the supersolid phases in binary Rydberg-dressed Bose-Einstein condensates

C.-H. Hsueh,¹ Y.-C. Tsai,^{1,2} K.-S. Wu,³ M.-S. Chang,³ and W. C. Wu¹

¹*Department of Physics, National Taiwan Normal University, Taipei 11677, Taiwan*

²*Department of Physics, National Changhua University of Education, Changhua 50058, Taiwan*

³*Institute of Atomic and Molecular Sciences, Academia Sinica, Taipei 10617, Taiwan*

(Dated: September 27, 2018)

We show that the five possible ordered states in a quantum spin-1/2 system with long-range exchange interactions: Néel, ladder, Peierls, coincidence, and domain states, can be realized in a binary Rydberg-dressed BEC system in the supersolid phase. In such a system, blockade phenomenon is shown to also occur for pairs of different excited-state atoms, which results in similar intra- and inter-species long-range interactions between ground-state atoms. It suggests that a pseudo spin-1/2 system can be possibly formed in the ground state of ultracold rubidium.

Supersolid (SS) is a matter state which simultaneously possesses crystalline and superfluid (SF) properties. For the past four decades, SS states have been studied by a number of authors[1–3] and in 2004 it was first claimed that the SS state has been observed in a ⁴He system[4], although in a later paper[5] some inconsistency was reported. An alternative and excellent candidate in which supersolidity can be possibly observed is the atomic Bose-Einstein condensate (BEC) which is clean and experimentally easily controllable [6–10]. In particular, Rydberg dressed BEC poses a great potential to exhibit the SS state that is intimately related to their long-range interaction. Very recently it has been theoretically shown that SF-SS transition in the Rydberg dressed BEC system is of the first order[11].

On the other hand, two- or multi-component system is of its own merit for fundamental interest especially in regards to the role of the inter-species interaction. For example, two-component BEC systems have been investigated on various properties by a number of groups[12–18]. Since the first experiment of two coexisting condensates of two different hyperfine states of ⁸⁷Rb was realized in 1997[19] and as the Rydberg dressing technique is mature, it becomes possible to explore a SS state with internal degrees of freedom (SS with a basis or a SS superlattice). Without the long-range interaction, there are basically two phases: miscible and insoluble, in a two-component SF system. With the long-range interactions, it is interesting to see how the SS states behave, which should provide a unique opportunity to study the complex phases of the two interpenetrating quantum crystals.

This Letter attempts to investigate the ground-state phase diagram of a binary Rydberg-dressed BEC system in the SS regime. It will be shown that five distinct phases of the SS structures are identified to exist in such a system. Of particular interest, these ground-state phases are in a strong analogy with the five possible spin orders in a quasi-two-dimensional quantum spin-1/2 system with long-range exchange interactions. Thus it suggests that a pseudo spin-1/2 system can be possibly formed in the ground state of ultracold ⁸⁷Rb.

Fig. 1(a) shows schematically a binary Rydberg-dressed

BEC system formed by two two-photon mechanisms. The binary system can be comprised of two different (hyper-fine) ground-state atoms excited to high-level Rydberg states. Alternatively, the system can also be possibly formed by exciting the same ground-state atoms to two different Rydberg states. Under the rotating-wave approximation, the interaction Hamiltonian of the system can be written as

$$\begin{aligned} \hat{H} = & \sum_{i < j} V^{(11)}(r_{ij}) \hat{\sigma}_{ee}^{(i)} \hat{\sigma}_{ee}^{(j)} - \hbar \Delta_1 \sum_i \hat{\sigma}_{ee}^{(i)} \\ & + \sum_{k < l} V^{(22)}(r_{kl}) \hat{\sigma}_{e'e'}^{(k)} \hat{\sigma}_{e'e'}^{(l)} - \hbar \Delta_2 \sum_k \hat{\sigma}_{e'e'}^{(k)} \\ & + \sum_{i,k} V^{(12)}(r_{ik}) \hat{\sigma}_{ee}^{(i)} \hat{\sigma}_{e'e'}^{(k)} + \hat{H}_1 + \hat{H}_2, \end{aligned} \quad (1)$$

where i, j, k, l are particle indices and $\hat{\sigma}_{\alpha\beta}^{(i)} \equiv |\alpha_i\rangle \langle \beta_i|$ define the corresponding transition and projection operators with $\alpha, \beta = e, g, e', g'$ denoting the excited and ground states of the first and the second species. $V^{(pq)}(r) = C_6^{(pq)}/r^6$ ($p, q = 1, 2$) are, at a distance r , the van der Waals (vdW) interactions between two identical/diverse Rydberg atoms and Δ_1, Δ_2 are the laser detunings. $\hat{H}_1 \equiv (\hbar\Omega_1/2) \sum_i [\hat{\sigma}_{ge}^{(i)} + \hat{\sigma}_{eg}^{(i)}]$ and $\hat{H}_2 \equiv (\hbar\Omega_2/2) \sum_k [\hat{\sigma}_{g'e'}^{(k)} + \hat{\sigma}_{e'g'}^{(k)}]$ with Ω_1, Ω_2 the Rabi frequencies, are to be treated as perturbations for $\Omega_1 \ll \Delta_1$ and $\Omega_2 \ll \Delta_2$ of interest. The interactions between ground-state atoms as well as between Rydberg- and ground-state atoms are ignored as they are not important for the studies. The effect of the foregoing interactions can be described in terms of a s -wave scattering pseudopotential[6].

The interaction potential between two identical/diverse dressed atoms can be well approximated by the Born-Oppenheimer (BO) energy surface W_G , which can be determined from a many-body perturbation expansion. Up to the fourth order involving couplings only to the singly and doubly excited many-body states: $|GG'\rangle = |G\rangle \otimes |G'\rangle$, $|E_i G'\rangle = |E_i\rangle \otimes |G'\rangle$, $|E_{ij} G'\rangle = |E_{ij}\rangle \otimes |G'\rangle$, $|GE'_i\rangle = |G\rangle \otimes |E'_i\rangle$, $|GE'_{ij}\rangle = |G\rangle \otimes |E'_{ij}\rangle$, and

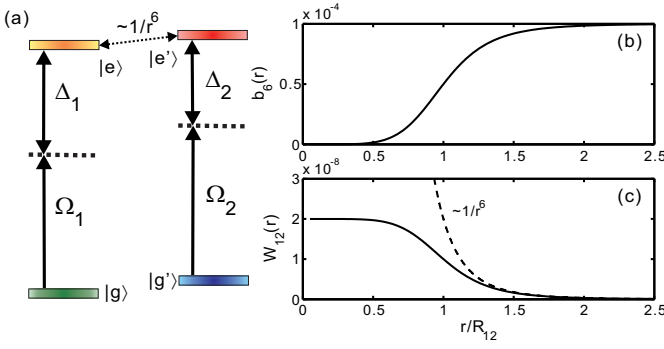


FIG. 1. (a) Schematic plot of a binary Rydberg-dressed BEC system with the emphasis of the additional vdW interaction between different-species excited atoms. Frame (b) shows the blockade phenomenon between different excited atoms by plotting the coefficient b_6 vs. the distance r (in units of R_{12}). Frame (c) shows the spatial dependence of the long-range interaction between different ground-state atoms by plotting the function W_{12} vs. r , in units of $\hbar\Delta_1$ [6].

$|E_i E'_j\rangle = |E_i\rangle \otimes |E'_j\rangle$, where $|G\rangle \equiv \otimes_k |g_k\rangle$, $|E_i\rangle \equiv |e_i\rangle \otimes_{k \neq i} |g_k\rangle$, $|E_{ij}\rangle \equiv |e_i e_j\rangle \otimes_{k \neq i,j} |g_k\rangle$, $|G'\rangle \equiv \otimes_k |g'_k\rangle$, $|E'_i\rangle \equiv |e'_i\rangle \otimes_{k \neq i} |g'_k\rangle$, and $|E'_{ij}\rangle \equiv |e'_i e'_j\rangle \otimes_{k \neq i,j} |g'_k\rangle$, we obtain

$$W_G = \sum_{i < j} W_{11}(r_{ij}) + \sum_{k < l} W_{22}(r_{kl}) + \sum_{i,k} W_{12}(r_{ik}) + \text{constant}, \quad (2)$$

where $(p, q = 1, 2)$ [6]

$$W_{pq}(r) = \frac{\tilde{C}_6^{(pq)}}{R_{pq}^6 + r^6}. \quad (3)$$

Here $\tilde{C}_6^{(pq)} = \nu_p \nu_q C_6^{(pq)}$ and $R_{pq} = [C_6^{(pq)} / (2\hbar\Delta_{pq})]^{1/6}$ with $\nu_l \equiv (\Omega_l / 2\Delta_l)^2$ ($l = 1, 2$), $\Delta_{11} \equiv \Delta_1$, $\Delta_{22} \equiv \Delta_2$, and $\Delta_{12} \equiv (\Delta_1 + \Delta_2)/2$ are the intra- and inter-species effective coupling constant and blockade radius, respectively. In the weak Rabi frequency limit of interest, $\nu_1, \nu_2 \ll 1$, the whole dressed state can be expressed as a direct product of two individual dressed states:

$$|\Psi\rangle = |\Psi_1\rangle \otimes |\Psi_2\rangle \approx b_1 |gg\rangle \otimes |g'g'\rangle + \frac{b_2}{\sqrt{2}} (|ge\rangle + |eg\rangle) \otimes |g'g'\rangle + b_3 |ee\rangle \otimes |g'g'\rangle + \frac{b_4}{\sqrt{2}} |gg\rangle \otimes (|g'e'\rangle + |e'g'\rangle) + b_5 |gg\rangle \otimes |e'e'\rangle + \frac{b_6}{2} (|ge\rangle + |eg\rangle) \otimes (|g'e'\rangle + |e'g'\rangle), \quad (4)$$

where the coefficients b_1 to b_6 are of order 1, $\sqrt{\nu_1}$, $\sqrt{\nu_2}$, ν_1 , ν_2 , and $\sqrt{\nu_1 \nu_2}$, respectively. Fig. 1(b) plots b_6 as a function of the distance r . It indicates clearly that the blockade effect also exists between the diverse excited Rydberg atoms. This in turn leads to similar intra- and inter-species long-range interactions between ground-state atoms, as shown explicitly by the plot of the inter-species potential W_{12} in Fig. 1(c).

As this paper concerns about the SS ground-states not too close to the SF-SS transition, mean-field Gross-Pitaevskii (GP) treatment should be sufficient for the study. In the dimensionless scheme, the GP energy functional of the system can be written as

$$E = E_0 + E_{\text{int}}, \quad (5)$$

where the single-particle part

$$E_0 = \sum_{i=1,2} \int d\vec{\rho} \left[|\nabla \psi_i(\vec{\rho})|^2 / 2 + \rho^2 |\psi_i(\vec{\rho})|^2 / 2 \right] \quad (6)$$

and the interaction part

$$E_{\text{int}} = \frac{1}{2} \sum_{i,j=1,2} \int d\vec{\rho} d\vec{\rho}' V_{ij}(\vec{\rho}) |\psi_i(\vec{\rho})|^2 |\psi_j(\vec{\rho}')|^2 \quad (7)$$

with $\vec{\rho} \equiv |\vec{\rho} - \vec{\rho}'|$. In (7), the intra- and inter-species interactions comprised of contact and long-range parts are

isotropic and

$$V_{ij}(\vec{\rho}) = \gamma_{ij} \delta(\vec{\rho}) + U_{ij}(\vec{\rho}) = \gamma_{ij} \delta(\vec{\rho}) + \frac{\alpha_{ij}}{r_{ij}^6 + \vec{\rho}^6}, \quad (8)$$

where $\alpha_{ij} = m \tilde{C}_6^{(ij)} / (\hbar^2 l_h^4)$ are the strengths of the long-range interactions, $r_{ij} = R_{ij} / l_h$ are the blockade radii, and $\gamma_{ij} = 4\pi a_{ij}$ are the two-dimensional coupling constants with a_{ij} the effectively s -wave scattering lengths. In Eqs. (6) and (7), it is assumed that the two-species Rydberg-dressed BECs are trapped respectively in the harmonic potentials $U_{\text{trap}}^{(i)} = m_i \omega_i^2 (\rho^2 + \lambda_i^2 z^2) / 2$ ($i = 1, 2$) in the cylindrical coordinates $\mathbf{r} = (\rho, \phi, z)$ with ω_i and λ_i being the radius frequencies and the aspect ratios, respectively. The length and energy scales are thus $l_h \equiv \sqrt{\hbar / m\omega}$ and $\hbar\omega$ respectively. Appropriate for the SS regime ($\lambda_i \gg 1$), the calculation is to be treated quasi-two-dimensionally and in this limit, the population is determined by $\int |\psi_i|^2 dx dy = N$ [20]. In actual calculations, for simplicity, it is assumed that $m_2 = m_1 \equiv m$, $\omega_2 = \omega_1 \equiv \omega$, and $\lambda_2 = \lambda_1 \equiv \lambda$. Moreover, we also assume that all the blockade radii r_{ij} are the same, labeled as r_c .

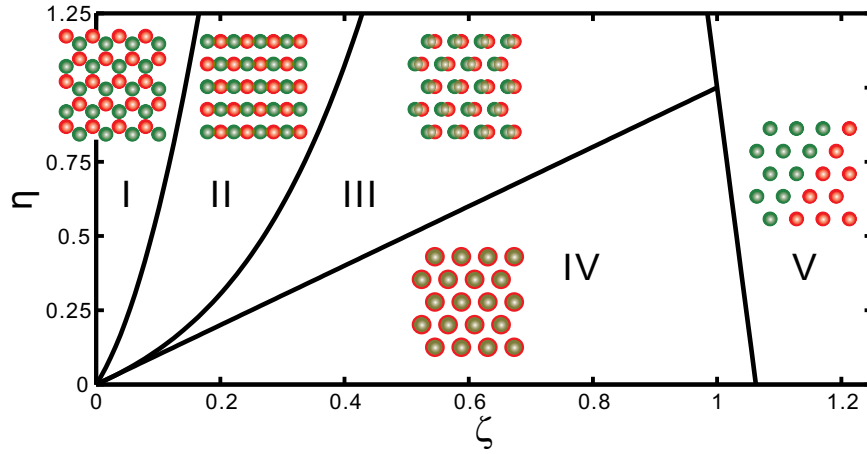


FIG. 2. Phase diagram of a binary Rydberg-dressed BEC system showing five distinct phases (I–V) in the SS regime. Considering green droplet to be a pseudospin up (\uparrow) and red droplet to be a pseudospin down (\downarrow), phase I–V correspond to Néel, ladder, Peierls, coincidence, and domain states in the quantum spin-1/2 system. ($\zeta = 1, \eta = 1$) is a tricritical point.

Fig. 2 shows the phase diagram of the system which is characterized by two parameters $\eta \equiv a_{12}/a_{11}$ and $\zeta \equiv \alpha_{12}/\alpha_{11}$ associated with the ratios of the short-range (contact) and long-range interactions respectively. Due to the robustness of the two hexagonal sublattices, five stable distinct phases (I)–(V) are unambiguously identified. In our calculations, the parameter space is first discretized into 40×20 points in the ζ - η plane. The phase boundaries are then carefully reexamined and demarcated between two neighboring phases. In terms of density structures (orders), they correspond to (I) honeycomb lattice (one droplet surrounded by three diverse ones), (II) rectangle lattice (one droplet surrounded by four diverse ones), (III) triangular lattice with dimeric basis, (IV) triangular lattice without basis, and (V) the domain structures. Demarcated by the $\eta = 1$ line, there are four and five phases above and below it, respectively. An explicit example of how density profiles behave in each phase is given in the top row of Fig. 3.

For the current two-species system, it is interesting and useful to introduce a two-component spinor wavefunctions, $\Psi \equiv (\psi_1, \psi_2)^t$. In terms of the “charge” $n \equiv \Psi^\dagger \sigma_0 \Psi = |\Psi_1|^2 + |\Psi_2|^2$ and the “spin” $n_s \equiv \Psi^\dagger \sigma_3 \Psi = |\Psi_1|^2 - |\Psi_2|^2$, the interaction energy functional in (7) can

be rewritten as

$$E_{\text{int}} = \frac{1}{4} \int d\vec{\rho} d\vec{\rho}' [V_{11}(\vec{\rho}) - V_{22}(\vec{\rho})] n(\vec{\rho}') n_s(\vec{\rho}) + \frac{1}{2} \int d\vec{\rho} d\vec{\rho}' J_s(\vec{\rho}) n_s(\vec{\rho}') n_s(\vec{\rho}) + \frac{1}{2} \int d\vec{\rho} d\vec{\rho}' J_n(\vec{\rho}) n(\vec{\rho}') n(\vec{\rho}), \quad (9)$$

where

$$J_n(\vec{\rho}), J_s(\vec{\rho}) = \frac{1}{4} [V_{11}(\vec{\rho}) + V_{22}(\vec{\rho}) \pm 2V_{12}(\vec{\rho})]. \quad (10)$$

The first term of E_{int} corresponds to a coupling between charge n and spin n_s , while the second and third terms correspond to spin and charge channels respectively. In the case $V_{11} \approx V_{22}$, the first term is negligible and thus the second and third terms dominate. In view of the second and third lines in (9), the spin-channel term has a strong analogy to the one for a spin liquid to which $J_s(\vec{\rho})$ is considered to be the corresponding *exchange* coupling. Whereas for the charge channel, $J_n(\vec{\rho})$ is considered to be the corresponding *Coulomb* interaction.

By separating out the contact and the long-range parts of the interaction and under the approximation $U_{11} = U_{22}$ and $U_{12} = \zeta U_{11}$ for the long-range part, the couplings in (10) can be rewritten as

$$J_n(\vec{\rho}), J_s(\vec{\rho}) = \frac{1}{2} [\gamma_{11} (1 \pm \eta) \delta(\vec{\rho}) + (1 \pm \zeta) U_{11}(\vec{\rho})]. \quad (11)$$

In view of (11) and considering the long-range effect in the

charge channel, the coefficient $1 + \zeta$ is always positive and it is the main cause for the robustness of the crystallization structure of the system[21–23]. More precisely, the robustness of the hexagonal sublattice for each species is due to the strong isotropic intra-species long-range interactions U_{11} and U_{22} . For the spin channel, in contrast, the coefficient $1 - \zeta$ is strongly magnitude and sign dependent. Consequently how the sublattices correlate with each other

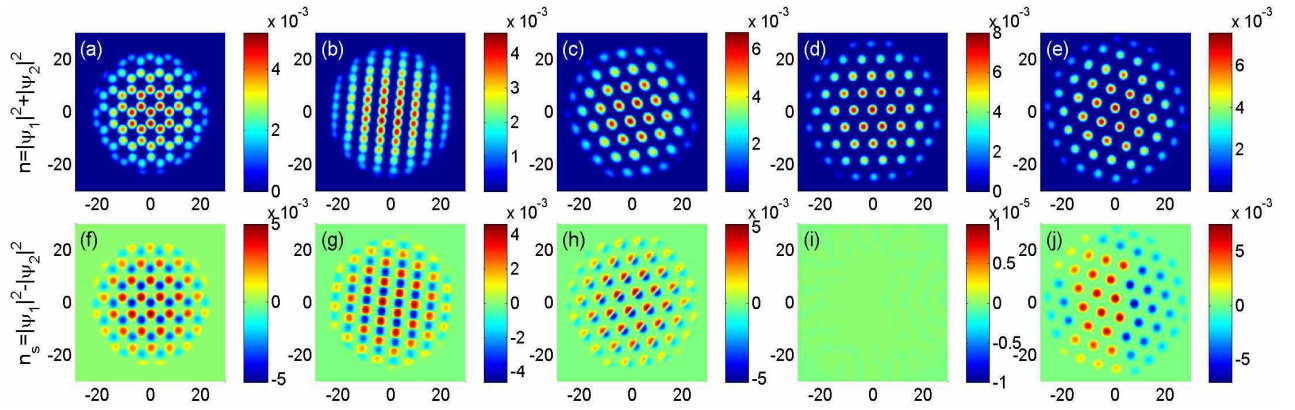


FIG. 3. Charge (top row) and spin (bottom row) orders of the five phases associated with a fixed $\eta = 0.75$ and $\zeta = 0.03125$ (a,f), 0.25 (b,g), 0.5 (c,h), 0.875 (d,i), and 1.25 (e,j) respectively. Other parameters used are $N\gamma_{11} = N\gamma_{22} = 10^4$, $r_c = 5$, and $N\alpha_{11} = N\alpha_{22} = 6.25 \times 10^7$.

will depend strongly on the value of ζ , or more precisely on the inter-species long-range interaction $U_{12} = \zeta U_{11}$.

The phase diagram in Fig. 2 can thus be alternatively interpreted in terms of spin orders (or magnetization) treating the system of pseudospin-1/2 [24]. With a relatively large and positive exchange coupling $\zeta' \equiv 1 - \zeta$, phase I corresponds to the Néel state on a honeycomb lattice. Phase II is so-called the n -leg spin-ladder state by relaxing the coupling ζ' . Phase III is the spin-Peierls state by further decreasing the coupling ζ' . Phase IV is the spin-up/spin-down coincidence state with relatively small but positive ζ' . Phase V is the domain state due to the sign change of the exchange coupling ($\zeta' < 0$). Moreover, based on the long-range exchange coupling given in Eq. (11), it is comprehended that when ζ' is positive, antiferromagnetism (AFM) dominates and as a matter of fact, the larger ζ or the smaller ζ' is, the more overlap between the two sublattices is. However, when ζ' changes sign to be negative, ferromagnetic (FM) dominates and consequently domains form. Therefore, one can classify phase I–IV belonging to AFM, while phase V belonging to FM. An explicit example of how the spin order behaves in each phase is given in the bottom row of Fig. 3.

Fig. 3 gives explicit examples of charge (top row) and spin (bottom row) orders associated with various phases in Fig. 2. A fixed $\eta = 0.75$ is used and ζ are varied to be 0.03125, 0.25, 0.5, 0.875, and 1.25 respectively for frame (a)&(f), (b)&(g), (c)&(h), (d)&(i), and (e)&(j), corresponding to phase I to V. Other parameters used are $N\gamma_{11} = N\gamma_{22} = 10^4$, $r_c = 5$, and $N\alpha_{11} = N\alpha_{22} = 6.25 \times 10^7$. Justifications of these parameters can be referred to Ref. [25] that warrants the validity of the blockade regime and the use of the effective long-range interactions.

By connecting the neighboring phases for a small and same ζ and by varying η , one is able to understand the role of the contact interactions. As a matter of fact, the increase of η (or the ratio of γ_{12}/γ_{11}) will increase the separation of the nearby diverse droplets, resulting in different lattices.

In summary, five distinct phases are identified to exhibit in the two-species Rydberg-dressed BEC system in the supersolid regime. These phases are in one-to-one correspondence to the five spin orders, Néel, ladder, Peierls, coincidence, and domain states in a quantum spin-1/2 system with long-range exchange interactions and suggest a possible pseudo spin-1/2 system forming in the ground state of rubidium.

We are grateful to Prof. Ming-Che Chang for many useful comments on this work. The supports from the National Science Council of Taiwan (under the grant No. NSC 99-2112-M-003-006-MY3) and the National Center of Theoretical Sciences of Taiwan are acknowledged.

-
- [1] A. F. Andreev and I. M. Lifshitz, *Sov. Phys. JETP* **29**, 1107 (1969).
 - [2] G. V. Chester, *Phys. Rev. A* **2**, 256 (1970).
 - [3] A. J. Leggett, *Phys. Rev. Lett.* **25**, 1543 (1970).
 - [4] E. Kim and M. H. W. Chan, *Nature (London)* **427**, 225 (2004); *Science* **305**, 1921 (2004).
 - [5] D. Y. Kim and M. H. W. Chan, *Phys. Rev. Lett.* **109**, 155301 (2012).
 - [6] N. Henkel, R. Nath, and T. Pohl, *Phys. Rev. Lett.* **104**, 195302 (2010).
 - [7] G. Pupillo, A. Micheli, M. Boninsegni, I. Lesanovsky, and P. Zoller, *Phys. Rev. Lett.* **104**, 223002 (2010).
 - [8] F. Cinti, P. Jain, M. Boninsegni, A. Micheli, P. Zoller, and G. Pupillo, *Phys. Rev. Lett.* **105**, 135301 (2010).
 - [9] S. Saccani, S. Moroni, and M. Boninsegni, *Phys. Rev. B* **83**, 092506 (2011).
 - [10] C.-H. Hsueh, T.-C. Lin, T.-L. Horng, and W. C. Wu, *Phys. Rev. A* **86**, 013619 (2012).
 - [11] T. Macri, F. Maucher, F. Cinti, and T. Pohl, preprint, arXiv:1212.6934.
 - [12] B. D. Esry and C. H. Greene, *Phys. Rev. A* **59**, 1457 (1999).
 - [13] M. Trippenbach, K. Góral, K. Rzkażewski, B. Malomed, and Y. B. Band, *J. Phys. B* **33**, 4017 (2000).

- [14] F. Riboli and M. Modugno, Phys. Rev. A **65**, 063614 (2002).
- [15] D. M. Jezek and P. Capuzzi, Phys. Rev. A **66**, 015602 (2002).
- [16] A. A. Svidzinsky and S. T. Chui, Phys. Rev. A **67**, 053608 (2003).
- [17] K. Kasamatsu, M. Tsubota, and M. Ueda, Phys. Rev. Lett. **91**, 150406 (2003).
- [18] C.-H. Hsueh, T.-L. Horng, S.-C. Gou, and W. C. Wu, Phys. Rev. A **84**, 023610 (2011).
- [19] C. J. Myatt, E. A. Burt, R. W. Ghrist, E. A. Cornell, and C. E. Wieman, Phys. Rev. Lett. **78**, 586 (1997).
- [20] When the Rydberg-dressed system is strongly confined in z -axis by a z -direction harmonic potential $(\omega\lambda)^2 z^2/2$ and relatively freely moving in the xy plane, the 3D wavefunction can be approximated by $\psi_i^{(3D)}(\mathbf{r}) = \psi_i^{(2D)}(\vec{\rho})\varphi_g(z)$ with $\varphi_g(z) = (\omega\lambda/\pi)^{1/4} \exp(-\omega\lambda z^2/2)$. As the softened range r_{ij} is much longer than the width of φ_g^2 , the 2D long-range interactions can be well approximated by $U_{ij}^{(2D)}(\vec{\rho} - \vec{\rho}') \approx \alpha_{ij}/[r_{ij}^6 + \bar{\rho}^6] \times \int \varphi_g(z)^2 \varphi_g(z')^2 dz dz' = \alpha_{ij}/[r_{ij}^6 + \bar{\rho}^6]$.
- [21] Mikael C. Rechtsman, Frank H. Stillinger, and Salvatore Torquato, Phys. Rev. Lett. **95**, 228301 (2005).
- [22] E. Edlund, O. Lindgren, and M. Nilsson Jacobi, Phys. Rev. Lett. **107**, 085503 (2011).
- [23] E. Edlund, O. Lindgren, and M. Nilsson Jacobi, Phys. Rev. Lett. **108**, 165502 (2012).
- [24] S. Blundell, Magnetism in Condensed Matter (Oxford 2001).
- [25] N. Henkel, F. Cinti, P. Jain, G. Pupillo, and T. Pohl, Phys. Rev. Lett. **108**, 265301 (2012).